

Nonisothermal reaction kinetics of diasporic bauxite

Haoqun Li^{a,b,*}, Tianmin Shao^b, Desheng Li^a, Darong Chen^b

^a *The College of Mechanical Engineering and Applied Electronics Technology, Beijing University of Technology, Beijing 100022, P.R. China*

^b *The State Key Laboratory of Tribology, Tsinghua University, Beijing 100084, P.R. China*

Received 3 June 2004; received in revised form 30 July 2004; accepted 6 August 2004

Available online 27 September 2004

Abstract

Thermogravimetric data for the decomposition of diaspore have been obtained under nonisothermal conditions. A model-free isoconversional method is used to yield dependency of the activation energy on the extent of conversion for experiments. Reaction model of the Sestak–Berggren equation is identified by Malek and Mitsuhashi method. The parameter of the model SB(m, n) and the pre-exponential factor (A) are calculated. © 2004 Elsevier B.V. All rights reserved.

Keywords: Diaspore; Kinetics; Nonisothermal; Decomposition; Arrhenius parameters

1. Introduction

Alumina is an important ceramic material used in various branches of industry. The most stable form of alumina is corundum (α -Al₂O₃), which has excellent properties such as high hardness, thermal resistance, corrosion resistance, etc. Alumina is chiefly obtained by the dehydroxylation of aluminum hydroxides. The transformations of boehmite (γ -AlOOH), gibbsite (γ -Al(OH)₃), and bayerite (α -Al(OH)₃) to corundum via a series of transition aluminas have been extensively studied [1–3]. By contrast, the transformation mechanism from diaspore (α -AlOOH) to corundum is not well understood. Diaspore is a major constituent of bauxite in Greece, Russia and China. In the United States, diaspore has also been found in clays in Missouri and Pennsylvania. It is commonly stated that diaspore directly transform into corundum at a relative low temperature due to the structural similarity of the phases, both having a hexagonally close packed anion sublattices [4]. A recent study reported that a two-step transformation with a new transition phase designated α' -Al₂O₃ occurred under vacuum and a possible mechanism by which diaspore is dehydrated to form α' -Al₂O₃ was presented

[5]. Therefore, the thermodecomposition kinetic properties of diaspore are of significance to the understanding of transformation mechanism and to Bayer's industry process.

The governing equation for kinetic analysis of solid-state decompositions

$$\frac{d\alpha}{dt} = k(T)f(\alpha) \quad (1)$$

where t is the time and T the temperature and α the extent of conversion, makes the implicit assumption that the temperature dependence of the rate constant, $k(T)$, can be separated from the reaction model, $f(\alpha)$. The reaction model may take various forms, some of which are given in Table 1. The explicit temperature dependence of the rate constant is introduced by replacing $k(T)$ with the Arrhenius equation, which gives

$$\frac{d\alpha}{dt} = A \exp\left(\frac{-E}{RT}\right) f(\alpha) \quad (2)$$

where A (the pre-exponential factor) and E (the activation energy) are Arrhenius parameters and R the gas constant. Under nonisothermal conditions in which samples are heated at a constant rate, the explicit temporal dependence of Eq.

* Corresponding author. Tel.: +86 1067396187; fax: +86 1067391331.
E-mail address: lihaoqun@bjut.edu.cn (H. Li).

Table 1
Set of reaction models applied to describe thermal decomposition in solids

No.	Reaction model	$f(\alpha)$	$g(\alpha)$
1	Power law	$4\alpha^{3/4}$	$\alpha^{1/4}$
2	Power law	$3\alpha^{2/3}$	$\alpha^{1/3}$
3	Power law	$2\alpha^{1/2}$	$\alpha^{1/2}$
4	Power law	$2/3\alpha^{-1/2}$	$\alpha^{3/2}$
5	One-dimensional diffusion	$1/2\alpha^{-1}$	α^2
6	First-order (Mampel)	$1 - \alpha$	$-\ln(1 - \alpha)$
7	Avrami–Erofeev	$4(1 - \alpha)[-\ln(1 - \alpha)]^{3/4}$	$[-\ln(1 - \alpha)]^{1/4}$
8	Avrami–Erofeev	$3(1 - \alpha)[-\ln(1 - \alpha)]^{2/3}$	$[-\ln(1 - \alpha)]^{1/3}$
9	Avrami–Erofeev	$2(1 - \alpha)[-\ln(1 - \alpha)]^{1/2}$	$[-\ln(1 - \alpha)]^{1/2}$
10	Three-dimensional diffusion	$3/2(1 - \alpha)^{2/3}[1 - (1 - \alpha)^{1/3}]^{-1}$	$[1 - (1 - \alpha)^{1/3}]^2$
11	Contracting sphere	$3(1 - \alpha)^{2/3}$	$1 - (1 - \alpha)^{1/3}$
12	Contracting cylinder	$2(1 - \alpha)^{1/2}$	$1 - (1 - \alpha)^{1/2}$

(2) can be eliminated through the trivial transformation

$$\frac{d\alpha}{dT} = \frac{A}{\beta} \exp\left(\frac{-E}{RT}\right) f(\alpha) \quad (3)$$

where $\beta = dT/dt$ is the heating rate.

Compared with isothermal experiments, nonisothermal runs are more convenient to carry out without a sudden temperature jump of the sample at the beginning. The commonly used methods that involve fitting experimental data to assumed forms of the reaction model fails to produce trustworthy kinetic information for nonisothermal experiments [6]. The reason arises from that “model-fitting methods” do not achieve a clean separation between the temperature dependence, $k(T)$, and the reaction model, $f(\alpha)$. It also arises partly because many reactions follow complex mechanisms involving multiple series or parallel steps with different activation energies. Therefore, model-fitting methods, which are aimed at extracting a single value of the activation energy for an overall process, are unable to reveal this type of complexity [7]. However, the “model-free isoconversional methods” can be used to eliminate the aforementioned drawbacks of model-fitting [8,9]. These methods allow the activation energy to be determined as a function of the extent of conversion and/or temperature without making any assumptions about the reaction model.

In this paper, we present kinetic analysis of thermal decomposition of diasporic bauxite by isoconversional methods.

2. Experimental

The bulk diasporic bauxite is firstly ground to particle size of about 10 μm , then treated by acid washing, filtration and desiccation (120 $^{\circ}\text{C}$). The element composition of the samples is analyzed using EDX of scanning electron microscopy (CSM 950, Opton). The results are shown in Table 2 (hydrogen cannot be detected by the as-used instrument). The element Ti exists in the form of both anatase and rutile, which do not have phase transformations in the temperature range investigated. The same is true for the elements Si and Fe, which take the form of Illite.

Table 2
Element composition of the samples

Element	O	Al	Si	Ti	Fe
Weight %	49.69	42.67	1.13	4.93	1.59
Atomic %	63.92	32.55	0.83	2.12	0.59

The thermogravimetric analysis (TGA) experiments are carried out using a high-temperature thermal analysis instrument (Model TGA92). The TG sensitivity of the instrument is 0.001 mg, and DTA sensitivity is 1 mV. Spectral pure Al_2O_3 powders are used as the reference. Samples of the as-treated powders are placed in platinum crucibles and heated in a flowing atmosphere of nitrogen. The instrument is programmed to heat the sample from room temperature at a constant heating rate. The programmed linear heating rates are established after an initial period of nonlinear heating. The actual heating rates used in the kinetic analysis, 3.01, 7.68, 10.13 and 14.87 K/min, are calculated from temperature measurements made during the actual period of decomposition. Buoyancy has been subtracted from the actual mass loss data.

3. Kinetic computations

3.1. Dependency of the activation energy on the extent of conversion

Rearrangement and integration of Eq. (3) for nonisothermal conditions gives

$$g(\alpha) = \frac{A}{\beta} \int_0^{T_\alpha} \exp\left(\frac{-E}{RT}\right) dT = \frac{AI(E, T)}{\beta} \quad (4)$$

where $I(E, T)$ is the temperature integral. Because $g(\alpha)$ is independent of the heating rate, Eq. (4) can be written for a given conversion and a set of experiments performed under different heating rates $\beta_i (i = 1, \dots, n)$ as follow [9]

$$\frac{A_\alpha I(E_\alpha, T_{\alpha,1})}{\beta_1} = \frac{A_\alpha I(E_\alpha, T_{\alpha,2})}{\beta_2} = \dots = \frac{A_\alpha I(E_\alpha, T_{\alpha,n})}{\beta_n} \quad (5)$$

Therefore, the activation energy can be determined at any particular value of α by finding the value of E_α for which the function [9]

$$\sum_{i=1}^n \sum_{j \neq i}^n \frac{I(E_\alpha, T_{\alpha,i})/\beta_i - I(E_\alpha, T_{\alpha,j})/\beta_j}{I(E_\alpha, T_{\alpha,j})/\beta_j} \quad (6)$$

is a minimum. The minimization procedure is repeated for each value of α to find the dependence of the activation energy on the extent of conversion. The values of $I(E, T)$ can be found by numerical integration using Romberg rule [10].

3.2. Reaction model and pre-exponential factor

Once the activation energy has been determined, it is possible to find the kinetic model which best describes the measure set of TA data. It can be shown that for this purpose it is useful to define two special functions $y(\alpha)$ and $z(\alpha)$, which can easily be obtained by simple transformation of experimental data [11–13], these functions can be expressed as follows

$$y(\alpha) = \left(\frac{d\alpha}{dt} \right) e^x \quad (7)$$

$$z(\alpha) = \pi(x) \left(\frac{d\alpha}{dt} \right) \frac{T}{\beta} \quad (8)$$

where $x = E/RT$, $\pi(x)$ is an approximation of the temperature integral. It has been verified that the shape of the $y(\alpha)$ function, as well as the maximum α_m of the $y(\alpha)$ function and α_p^∞ of the function $z(\alpha)$, can be used to guide the choice of a kinetic model [11–13]. Knowing the value of the activation energy and the kinetic model, the pre-exponential factor can be calculated using the equation

$$A = -\frac{\beta x_p}{T_p f'(\alpha_p)} e^{x_p} \quad (9)$$

The value of activation energy used above is taken as an average in the $0.3 \leq \alpha \leq 0.7$ range. This is known as the Malek and Mitsuhashi method [14].

4. Results and discussion

The thermogravimetric curves in nonisothermal conditions are obtained at various heating rates. The experimental $\alpha - T$ plots which are analysed by isoconversional method (Eqs. (4)–(6)) are shown in Fig. 1. This method enables plotting of apparent activation energy E_α as shown in Fig. 2. It can be seen that the activation energy is practically independent of the value of α in the $0.2 < \alpha < 0.8$ range (with a average value of about 175 kJ mol^{-1}), but is somewhat lower in both the early and terminal stages of the reaction, which may indicate a multi-step mechanism of decomposition of diaspore.

The most probable kinetic model can be determined using the $y(\alpha)$ and $z(\alpha)$ functions. These functions are obtained

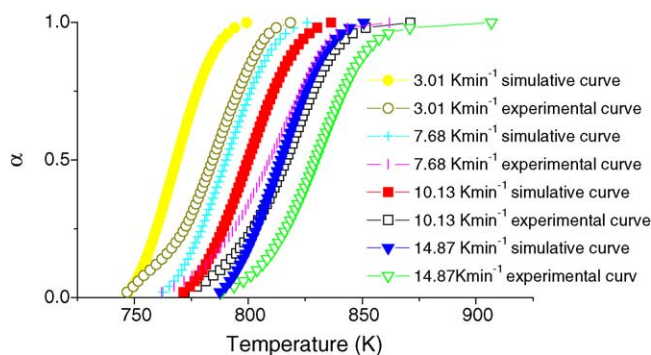


Fig. 1. Experimental alpha-temperature curves vs. simulative curve obtained by Sestak-Berggren model at different heating rates.

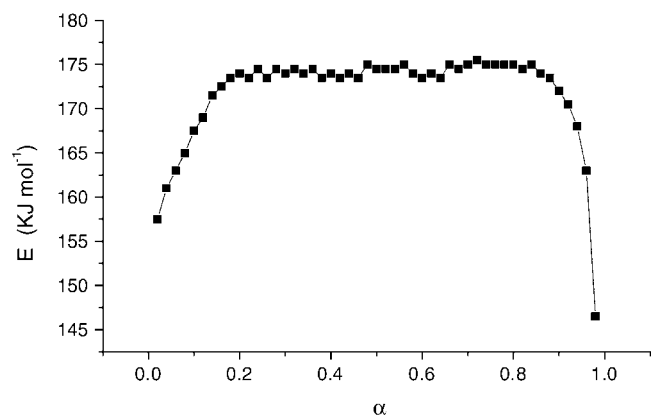


Fig. 2. Dependency of the activation energy on extent of conversion determined using the model-free isoconversional technique.

using Eqs. (7) and (8) and they are shown in Figs. 3 and 4, respectively. The values of α_m and α_p^∞ corresponding to the maxima of both $y(\alpha)$ and $z(\alpha)$ curves are summarized in Table 3. It is evident that the values of these important parameters conform to the SB(m, n) model [15], which is known as:

$$f(\alpha) = \alpha^m (1 - \alpha)^n \quad (10)$$

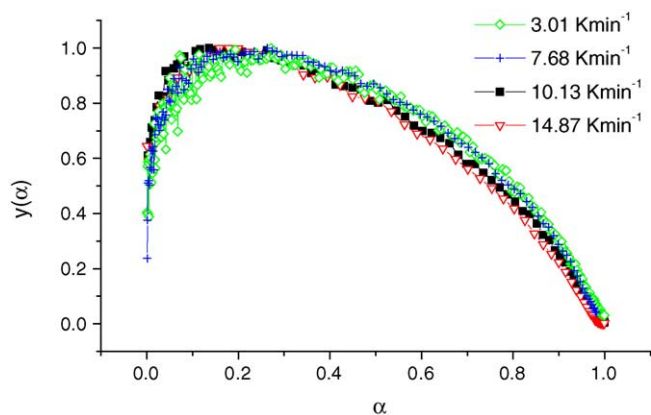


Fig. 3. The $y(\alpha)$ functions calculated using Eq. (7) for experiments at various heating rates.

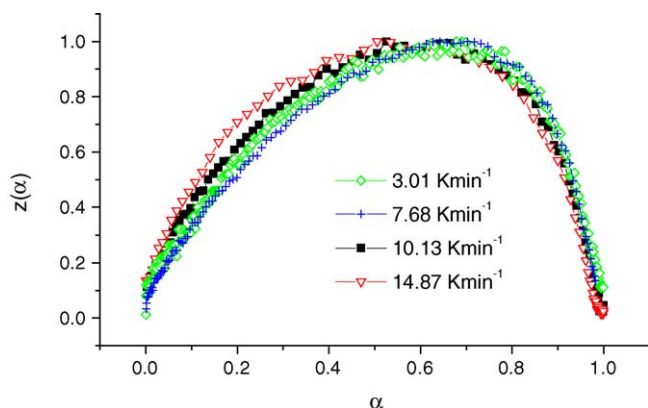


Fig. 4. The $z(\alpha)$ functions calculated using Eq. (8) for experiments at various heating rates.

Table 3
The values of α_m and α_p^∞

β (K min ⁻¹)	α_m	α_p^∞
3.01	0.271	0.678
7.68	0.263	0.702
10.13	0.136	0.525
14.87	0.179	0.505

Table 4
The kinetic parameters obtained using Malek method and constant value of activation energy (175 kJ mol⁻¹)

β (K min ⁻¹)	m	n	ln A (min ⁻¹)
3.01	0.269	0.722	24.28
7.68	0.276	0.772	24.16
10.13	0.106	0.673	24.82
14.87	0.171	0.784	24.91

The kinetic parameter ratios = m/n can be calculated using the equation

$$s = \frac{\alpha_m}{1 - \alpha_m} \quad (11)$$

Then Eq. (2) may be expressed in the form

$$\ln \left(\frac{d\alpha}{dt} \exp \left(\frac{E}{RT} \right) \right) = \ln A + n \ln [\alpha^s(1 - \alpha)] \quad (12)$$

The kinetic parameter n corresponds to the slope of linear dependence of $\ln[(d\alpha/dt) \exp(E/RT)]$ versus $\ln[\alpha^s(1 - \alpha)]$. Then the second kinetic exponent is $m = s \times n$. The results calculated are shown in Table 4. Taking these values we can calculate average kinetic parameters for the decomposition of diaspor as follows: $E = 175 \text{ kJ mol}^{-1}$, $\ln A = 25 \text{ min}^{-1}$, $m = 0.205$, $n = 0.738$.

On the basis of the assessment of E , A , m and n as shown above, the simulative $\alpha - T$ plots can be obtained using the

Eq. (3). The simulative transformation curves at the same heating rates are shown in Fig. 1. It is obvious that there are some deviations between simulative and experimental curves. The reasons may lie in the following aspects. Firstly, the value of activation energy used is taken as an average in the $0.3 \leq \alpha \leq 0.7$ range which may be different from the actual value. Other model-free methods of analysis of activation energy may be used as comparison in the next work. Secondly, the assessment of A , m and n is also average value of the four heating rates. This deviation may be inevitable in Malek method.

Thirdly, the absolute linear heating rates are impossible in the whole experimental process; that is to say, the experimental transformation curves are not as accurate as they should be. To sum up, much work may need to be done for solid-state kinetics.

5. Conclusions

The kinetic process for the decomposition of diaspor under nonisothermal conditions has been studied. The model-free isoconversional method is used to yield dependency of the activation energy on the extent of conversion and Malek and Mitsunashi method is used to identify the most probable kinetic model. It is established that the decomposition of diaspor is a multi-step mechanism and can be described by the Sestak–Berggren model with the kinetic parameters as follows: $E = 175 \text{ kJ mol}^{-1}$, $\ln A = 25 \text{ min}^{-1}$, $m = 0.205$, $n = 0.738$.

References

- [1] C. Novak, G. Pokol, V. Izvekov, J. Therm. Anal. 36 (1990) 1895–1909.
- [2] M. Pyzalski, M. Wojcik, J. Therm. Anal. 36 (1990) 2147–2151.
- [3] M. Halvarsson, S. Vuorinen, Surf. Coat. Technol. 76/77 (1995) 287–296.
- [4] G. Ervin Jr., Acta Crystallogr. 5 (1952) 103–109.
- [5] A.H. Carim, G.S. Rohrer, N.R. Dando, J. Am. Ceram. Soc. 80 (1997) 2677–2680.
- [6] S. Vyazovkin, C.A. Wight, Annu. Rev. Phys. Chem. 48 (1997) 125–149.
- [7] S. Vyazovkin, C.A. Wight, J. Phys. Chem. A 101 (1997) 8279–8284.
- [8] S. Vyazovkin, C.A. Wight, Thermochim. Acta 340/341 (1999) 53–68.
- [9] S. Vyazovkin, J. Therm. Anal. 49 (1997) 1493–1499.
- [10] R.Z. Hu, Q.Z. Shi, Kinetics of Thermal Analysis, 1st ed., Science Press, Beijing, 2001.
- [11] J. Malek, Thermochim. Acta 138 (1989) 337–346.
- [12] J. Malek, Thermochim. Acta 200 (1992) 257–269.
- [13] S. Montserrat, J. Malek, P. Colomer, Thermochim. Acta 313 (1998) 83–95.
- [14] M.E. Brown, M. Maciejewski, S. Vyazovkin, et al., Thermochim. Acta 355 (2000) 125–143.
- [15] J. Sestak, Thermophysical Properties of Solid-state, Elsevier, Amsterdam, 1980.